Arch. Metall. Mater. **68** (2023), 4, 1349-1355

DOI: https://doi.org/10.24425/amm.2023.146200

K.A.A. HALIM[1,2*], J.E. KENNEDY[3], M.A.A. M. SALLEH[1,2], A.F. OSMAN[1,2], M.F. OMAR[1,2], N.M. SUNAR[4]

MICROMECHANICAL MODELING OF POLYAMIDE 11 NANOCOMPOSITES PROPERTIES USING COMPOSITE THEORIES

The use of organically modified clays as nano-reinforcement in polymer matrices is widely investigated owing to their remarkable reinforcement at low filler loading. In this body of work, the nanocomposites were prepared by melt blending nanoclay with polyamide 11 (PA 11) utilising a twin-screw extruder in order to maximise the dispersion of clay particles within the matrix during compounding. The main aim of the work was to study the reinforcing effect of nanoclay within PA 11 using two micromechanical model namely Halpin-Tsai and Mori-Tanaka composite theories. These theories were used to predict the effective tensile modulus of PA 11 nanocomposites and the results were compared to the experimental data. In addition, the Halpin-Tsai model was used to predict the storage modulus and heat distortion temperature (HDT) of PA 11 nanocomposites. It was found that the tensile modulus for nanocomposites with a high clay aspect ratio exhibits up to 10% higher when compared to the nanocomposites with lower clay aspect ratio. Thus, it is believed that the combination of clay aspect ratio and modulus contributes to the super reinforcing effect of nanoclay within the PA 11 matrix.

Keyword: Polymer nanocomposites; composite theories; melt blending; micromechanical model; Halpin-Tsai; Mori-Tanaka; heat distortion temperature

1. Introduction

Polymer layered silicates have attracted the wide attention of academia and industry over the past decades due to their exceptional reinforcement at very low filler loading than conventional fillers [1-4]. One of the major differences between layered silicates and conventional fillers is that the former has much larger surface area per unit volume compared to that the former has much larger surface area per unit volume than the latter. Thus, because of such larger surface area, layered silicates can be very efficient reinforcements since many important chemical and physical interactions are governed by the matrix and filler interface. For instance, studies have shown that the addition of 6.5 wt% layered silicates (nanoclays) within PA6 increased storage modulus by twofold; whereas, three times this amount of glass fibre is needed to achieve the same increase [5].

The presence of nanoclay platelet can significantly alter the properties of the polymer matrix. Layered silicates or nanoclays are composed of extremely thin (~1 nm) sheet like platelets with large surface areas and high aspect ratios. In addition, these platelets have a stiffness of approximately 178 GPa [5-7] compared to that of the polymer matrix. Therefore, due to the high surface area, aspect ratio and stiffness, the layered silicates can be very efficient reinforcements, in which the presence of nanoclay platelet can significantly alters. However, to achieve such reinforcing effect, the reinforcement efficiency of layered silicates strongly depends on the degree of dispersion of the nanoclay platelets and the structure of the nanocomposites [7]. In general, the polymer nanocomposites structures can be divided into three categories namely intercalated, partially intercalated/exfoliated and fully exfoliated [2,3,8]. The intercalated nanocomposites structure consists of polymer chains inserted between individual silicate layers. In contrast, for partially intercalated/exfoliated structures, the intercalated stacks and exfoliated layers are randomly distributed in the matrix. The layered nanoclay structure is disrupted for the fully exfoliated structure and the individual clay platelets are fully dispersed within the matrix. Ideally, the full exfoliation and dispersion of nanoclay platelets within

[1] UNIVERSITI MALAYSIA PERLIS, CENTRE OF EXCELLENCE GEOPOLYMER AND GREEN TECHNOLOGY (CEGEOGTECH), 01000 PERLIS, MALAYSIA
[2] UNIVERSITI MALAYSIA PERLIS, FACULTY OF CHEMICAL ENGINEERING AND TECHNOLOGY, KOMPLEKS PUSAT PENGAJIAN JEJAWI 3, KAWASAN PERINDUSTRIAN JEJAWI, 02600, ARAU, PERLIS, MALAYSIA
[3] ATHLONE INSTITUTE OF TECHNOLOGY, DUBLIN ROAD, CO. WESTMEATH, IRELAND
[4] UNIVERSITI TUN HUSSEIN ONN MALAYSIA, RESEARCH CENTRE FOR SOFT SOIL (RECESS), INSTITUTE OF INTEGRATED ENGINEERING, 86400 PARIT RAJA, JOHOR, MALAYSIA
* Corresponding author: kanwar@unimap.edu.my

the polymer matrix will lead to a maximum property improvement [9-11]. However, in most cases, only partial intercalation/exfoliation of nanocomposites structure can be achieved than fully exfoliated structure.

Overall, many factors could contribute to the property changes due to additions of layered silicates. The need for a better understanding of the relative contribution from each factor is inevitable. For instance, Zare et al. [12] uses a simple model to compare the values predicted against experimental for electrical conductivity of polymer cabon nanotubes (CNT). Navidfar and Trabzon [13] investigates the graphene type dependence of carbon nanotubes/graphene nanoplatelets polyurethane nanocomposites using micromechanical modeling. Furthermore, Sadeghpour et al [14] modified a model by incorporating filler-matrix interface failure to model graphene/polymer nanocomposites properties. Thus, modeling material properties is inevitable where it could provide valuable information on the underlying physics and the structure property relationships across diverse type of materials classification [15-17]. This study aims to evaluate whether the reinforcing effect of layered silicates within PA 11 can be explained using composite theories. The prediction stiffness of a unidirectional composite as a function of aspect ratio using established composite theory developed by Halpin and Tsai whereas the Mori-Tanaka model was derived on the principles of Eshelby's inclusion model for predicting an elastic stress field in and around and ellipsoidal particle in an infinite matrix. Moreover, this preliminary work attempts to model the PA 11 nanocomposites properties by employing both analytical models in order to investigate the effects of filler geometry and stiffness within the polymer matrix. Comparisons between the model predictions and the experimental mechanical data will be also reported. In addition, the heat distortion temperature (HDT) for PA 11 nanocomposites, based on dynamic mechanical data, will be presented and were compared to the theoretical predictions.

2. Experimental

The polymer used in this work was PA 11, Rilsan B, Besvoa, obtained from Arkema, France. The organically modified layered silicate used in this study was Cloisite 30B, a natural montmorillonite modified with a quaternary ammonium salt obtained from Southern Clay Products Co. USA. The PA 11 granules and Cloisite 30B nanoclay powder were dried in a Piovan DSN 504 desiccant drier at 80°C for 8 hours and at 75°C for 24 hours respectively prior to compounding. The nanocomposites were prepared by melt blending nanoclay with PA 11 and the compounding process was carried out on a Leistritz Micro 27 twin screw extruder. The nanocomposites subsequently injection moulded using ASTM D638 Type IV mould to prepare samples of suitable dimensions for mechanical testing.

The dispersion and nanoscale morphology of selected PA 11 nanocomposites was investigated by means of transmission electron microscopy (TEM). TEM was performed on samples from central region of tensile dumbbell specimen, normal to the injection flow (FD). The thickness and aspect ratio of the nanoclay particles was measured where the electron beam is parallel to both principal direction to the flow direction and transverse direction. A number of nanoclay fibers were examined to measure the aspect ratio of the dispersed nanoclay phase. Tensile testing of nanocomposites was performed on an Instron 3365 universal testing machine using a 5 kN load cell with a crosshead speed of 10 mm/min. Injection moulded Type IV dumbbell shape specimen was used and, in all cases, the test was carried out in accordance with ASTM 638 at ambient temperature. A minimum of 5 test specimens were tested from each batch. Dynamic mechanical analysis (DMA) studies were carried out using a TA DMQ-800 instrument in accordance with ASTM D6110. The test was carried out in single cantilever mode, using a sample of dimension 17 mm × 12 mm × 2 mm, over a wide temperature range from –130°C to 150°C. 1 Hz test frequency was used and a heating rate of 3°C/min was maintained. The heat distortion temperature (HDT) for the virgin and nanocomposite materials was estimated using the storage modulus data from DMA analysis based on a technique developed by Scobbo [18] and used by Fornes et al. [5].

Halpin-Tsai model

The Halpin-Tsai model is a well-known composite theory to predict the stiffness of unidirectional composites as a function of aspect ratio. This theory was developed from the generalised form of self-consistent model for a composite by considering a single fibre encased in a cylindrical shell of matrix, embedded in an infinite medium assumed to possess the average properties of the composite [5,19,20]. In this model, the longitudinal E_{11} and transverse E_{22} engineering moduli are expressed in the following general form [19-21];

$$\frac{E}{E_m} = \frac{1+\xi\eta\phi_f}{1-\eta\phi_f} \tag{1}$$

where E and E_m represent the Young's modulus of the composite and matrix, respectively, ϕ_f is the volume fraction of filler, and η is given by;

$$\eta = \frac{E_f / E_m - 1}{E_f / E_m + \xi_f} \tag{2}$$

where E_f represents the Young's modulus of the filler, ξ_f is the shape parameter which depends on the filler geometry and loading direction. When calculating the longitudinal modulus E_{11}, ξ_f is equal to $2(l/t)$ whereas for the transverse modulus, E_{22}, ξ_f is equal to $2(w/t)$. The parameters of l, w and t are the length, width and thickness of the dispersed fillers respectively.

Mori-Tanaka model

The Mori-Tanaka model [22,23] was derived on the principles of Eshelby's inclusion model for predicting an elastic stress field in and around and ellipsoidal particle in an infinite matrix. Tandon and Weng [24] used the Mori Tanaka approach to develop solutions for the elastic moduli of an isotropic matrix filled with spheroidal inclusions. The longitudinal and transverse moduli are expressed as follows;

$$\frac{E_{11}}{E_m} = \frac{A}{(A + \phi_f (A_1 + 2v_m A_2)} \tag{3}$$

$$\frac{E_{22}}{E_m} = \frac{1}{2A + \phi_f [-2v_o A_3 + (1 - v_m) A_4 + (1 + v_m) A_5 A} \tag{4}$$

where ϕ_f is the filler volume fraction, v_o is the poisons ratio of the matrix and A_1, A_2, A_3, A_4, A_5 and A are functions of the Eshelby's tensors.

3. Results and discussion

3.1. Determination of nano clay aspect ratio

The dispersion and orientation of nanoclay within the PA 11 matrix was analysed in detail using TEM. It was observed that the PA 11 grade used in this study promotes good exfoliation of Cloisite 30B nanoclay during melt compounding. The exfoliation of the nanoclay within PA 11 was primarily due to the separation of clay layers as a result of polymer chains insertion between the clay galleries which increased the interlayer spacing between the clay layers. Detailed morphological analysis of the injection moulded specimens revealed that the dispersed clay platelets exhibit a high degree of orientation along the flow direction as depicted in Fig. 1. The grayish regions and the dark lines as illustrated in Fig. 1 correspond to the polymer matrix and the clay platelets, respectively. The observation made on the TEM photomicrographs provides valuable information that will be used to model the nanocomposite systems using composite theory. However, in order to model these nanocomposites, the aspect ratio of the dispersed nanoclay platelets must be determined. The estimation of the clay platelets aspect ratio can be calculated by dividing the average particle length along the flow direction with the average particle thickness. The thickness of a perfectly exfoliated system is simply the thickness of a single clay platelet which is approximately 1 nm. Fig. 2(a), (b) illustrates the measurement of typical platelet thickness determined from intensity profiles for nanocomposite with 6 wt% clay loading. The histograms of clay particle number as function of aspect ratio for nanocomposites with 2 wt% and 6 wt% clay loading are shown in Fig. 3. These data were obtained by measuring number of clay particles from each nanocomposite samples. The average aspect ratio of PA 11 nanocomposites with 2 wt% and 6 wt% nanoclay loading were found to be 47.2 and 64.5

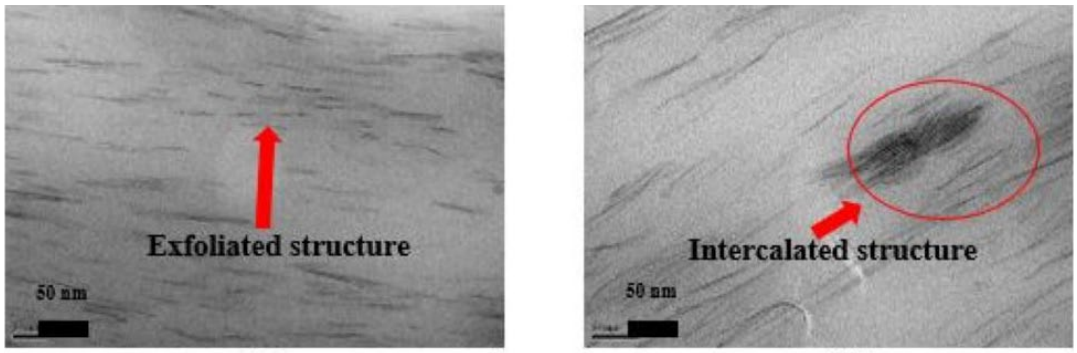

Fig. 1. TEM photomicrographs of PA 11 nanocomposites parallel to the flow direction; a) 2 wt% nanoclay, b) 6 wt% nanoclay

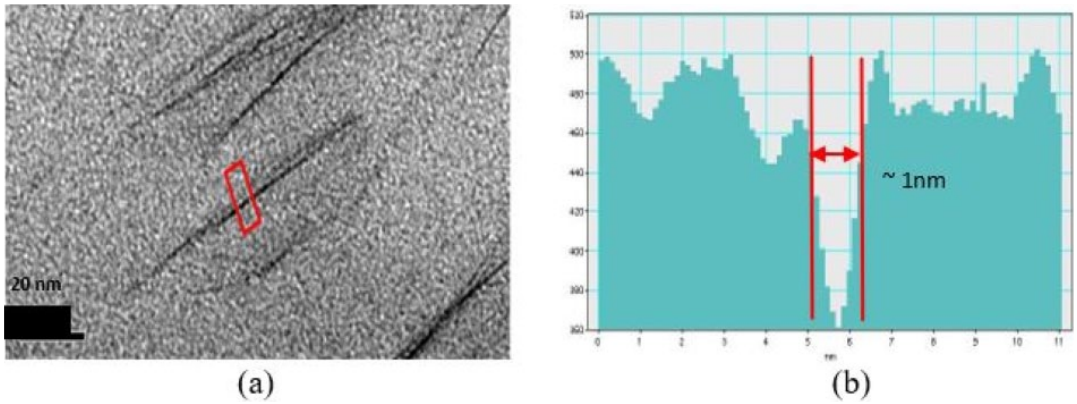

Fig. 2. Measurement of clay platelet thickness; a) typical fibre thickness, b) intensity profiles taken from the boxed region in (a)

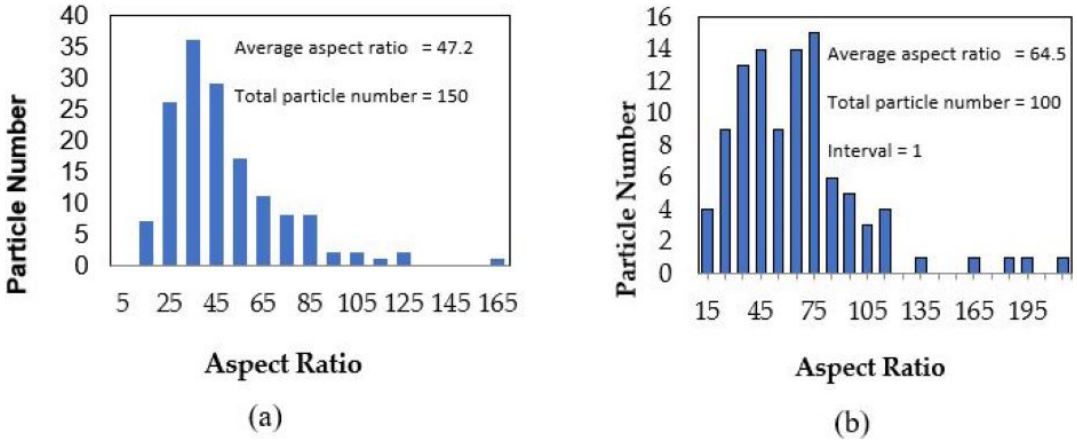

Fig. 3. Histograms of clay particle aspect ratio within PA 11 nanocomposites for (a) 2 wt% nanoclay, (b) 6 wt% nanoclay

respectively. Ideally, it is anticipated that the low aspect ratio can be observed at lower clay loading. Nevertheless, the higher aspect ratio observed at higher clay loading in this study was probably due to the combination of exfoliated and intercalated structures were measured during TEM analysis compared to only exfoliated structure observed at low clay loading.

3.2. Model calculations for PA 11 nanocomposites: Comparison between theoretical and experimental data

In this section, the extent of reinforcement of nanoclay platelets within PA 11 matrix was calculated using the Halpin-Tsai and Mori-Tanaka theories. The model predictions for the nanocomposites were compared against the experimental data. TABLE 1 lists the important material properties that were used for the modeling calculations. It is worth noting that the matrix and filler materials were assumed to be linear elastic and isotropic. The values of PA 11 and the filler modulus were taken from the values reported in the literature.

TABLE 1

Materials property data used in nanocomposite modeling [5,7,25,26]

Material	Young's Modulus (GPa)	Density (g/cm^3)	Poisson's ratio
PA 11	1.23	1.03	0.35
Cloisite 30B	178	1.98	0.20

Fig. 4 shows the effect of aspect ratio on the longitudinal reinforcement of PA 11 as calculated using the theories of Halpin-Tsai and Mori-Tanaka. In this case, the nanoclays within the nanocomposites were treated as fully exfoliated. With reference to Fig. 4(a), the increasing of aspect ratio from 47.2 to 64.5 leads to a significant increase in reinforcement efficiency as predicted by both theories. However, when comparing the experimental data for the PA 11 nanocomposites with the Halpin-Tsai model, it was found that the equations overpredict the experimental data. On the other hand, the modulus predictions using Mori-Tanaka

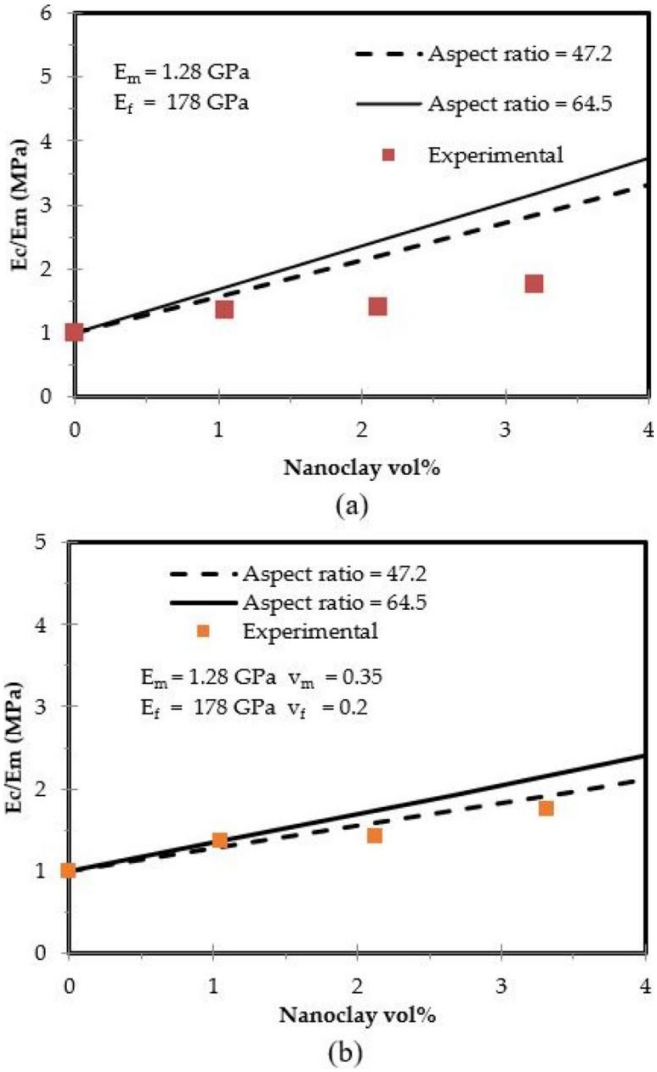

Fig. 4. Experimental and theoretical tensile modulus for PA 11 nanocomposites: a) Halpin Tsai, b) Mori-Tanaka based on longitudinal reinforcement

theory gives slightly different trends as shown in Fig. 4(b). As can be observed, the experimental data at low volume fraction of clay fall between the Mori-Tanaka predictions corresponding 47.2 and 64.5 aspect ratio, whereas, at higher clay concentration, the

theoretical predictions (at lower aspect ratio) were found to be close to the experimental values.

As mentioned earlier, the model calculations were based on an assumption that the nanocomposites systems were fully exfoliated. Nevertheless, evident from the TEM images, the exfoliations of clay platelets were significant at low clay loading; whereas, at high clay loading, a mixture between exfoliated and intercalated were presence. Therefore, the primary difference between the experimental value with the values obtained from the models was believed due to the structure formation within the nanocomposite systems. Overall, the Halpin-Tsai and Mori-Tanaka theories show that the predictions of nanocomposite modulus were dependent on the significant effects of filler modulus and aspect ratio. At high aspect ratio of clay fillers, the level of reinforcement for the nanocomposites is predicted to be higher than at low aspect ratio. These demonstrate that even higher levels of reinforcement can be achieved by higher level of clay exfoliation within the polymer matrix.

3.3. Theoretical prediction of storage modulus and heat distortion temperature (HDT)

The storage modulus data obtained from DMA can be used to estimate the HDT of a polymer. Since the HDT represents a temperature where a material exhibits a defined modulus, the Young's modulus, E, can be determined as follow;

$$E = \frac{\sigma_{max} L^2}{6\delta d} \quad (5)$$

where the σ_{max} is the maximum stress (1.82 MPa), d is the width of the sample, δ is the sum of initial deflection (typically 0.08 mm), and the deflection when HDT is registered (0.25 mm) and L is the length of span. To solve the E from the equation as mentioned above, the L and d were taken as 100 mm and 12.5 mm respectively. Figs. 5 and 6 illustrates the estimation of HDT at defined stress of 1.82 MPa and the estimated HDT values as a function of nanoclay loading respectively. With reference to Fig. 6, the estimated HDT of 41°C for virgin PA 11 was recorded where the value reported here was slightly lower to those reported in literature that is 50°C. Addition of 2 wt% nanoclay increased HDT of 13°C; whereas, at higher clay loading, in particular at 6 wt%, the HDT of the nanocomposite was increased almost two-fold compared to virgin PA 11. The significant increase in HDT is a result of increase in the storage modulus due to addition of the nanoclay, thus, reflecting the high reinforcing efficiency of the dispersed nanoclay.

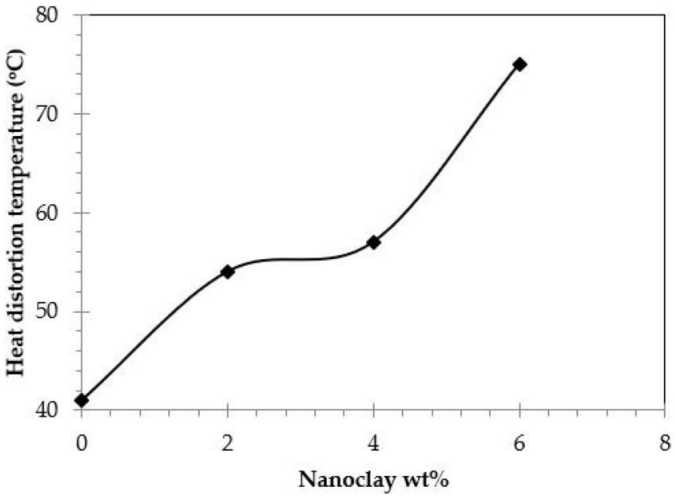

Fig. 6. Effect of nanoclay loading on the HDT for PA 11 nanocomposites

Fig. 7 shows the storage modulus predicted using Halpin Tsai equations which may be compared to the experimental plots in Fig. 5; whereas, Fig. 8 compares the HDT estimated from the experimental data with those predicted using Halpin-Tsai equations. As shown in Figure 8, the predicted HDT at low loading was comparable to the experimental data. However, at higher clay loading (6 wt%), the HDT was approximately 50°C higher than the estimation from the experimental data.

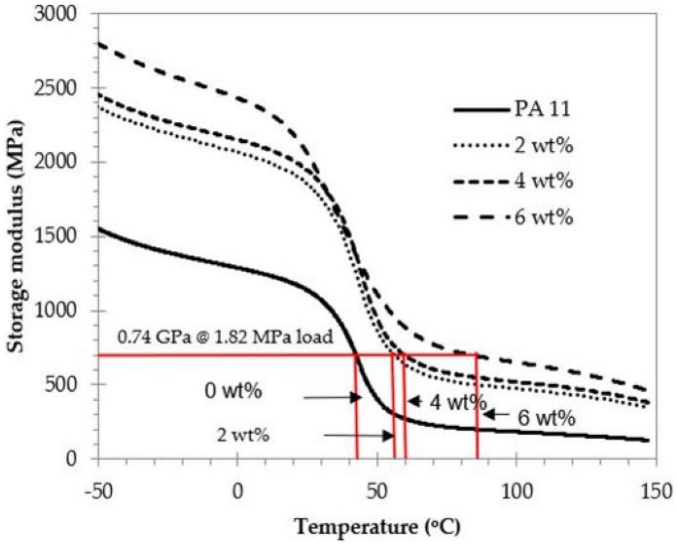

Fig. 5. Estimation of HDT values from experimental storage modulus data for PA 11 nanocomposites

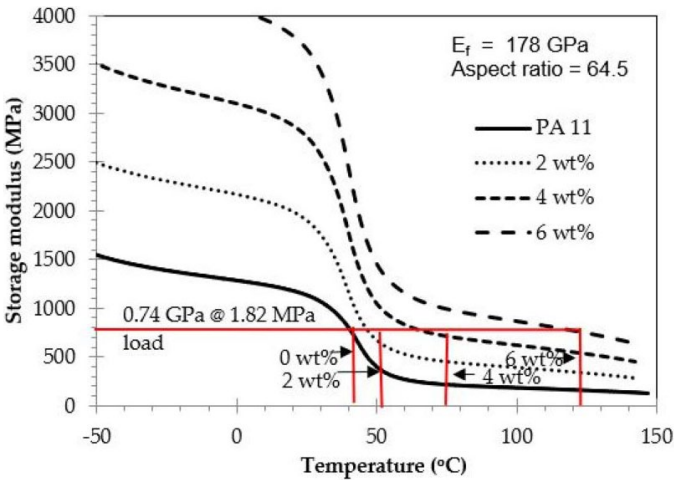

Fig. 7. Halpin-Tsai predictions for storage modulus as a function of temperature for all experimental nanoclay loadings

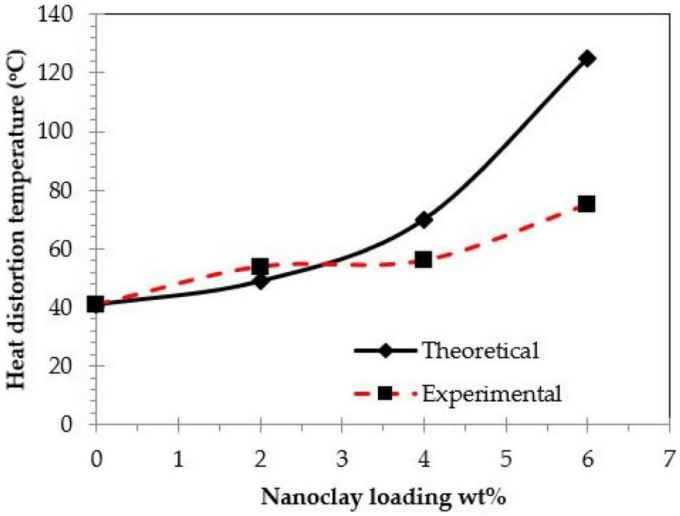

Fig. 8. HDT as a function of nanoclay loading for PA 11 nanocomposites

4. Conclusion

The Halpin-Tsai and Mori-Tanaka theories were employed to model the reinforcing efficiency of nanoclay within PA 11 matrix.

i. Based on the work carried out, it can be concluded that both theories showed on how the nanocomposites modulus responds to the filler aspect ratio and modulus although these theories were differed in terms of the treating the filler geometry.
ii. A higher aspect ratio leads to a higher composite modulus as predicted in both theories. It was found that the predictions of tensile modulus using Mori-Tanaka were close to the experimental values than the Halpin-Tsai model.
iii. The primary difference between the experimental value with the values obtained from the models was believed due to the structure formation within the nanocomposite systems. Further TEM studies of PA 11 nanocomposites at different loadings of nanoclay is essential in order to establish and understand the mechanism of structure formation within the nanocomposite systems.
iv. Concerning the estimation of HDT for PA 11 nanocomposites from DMA data, the predicted HDT using Halpin-Tsai model was found to be comparable at lower nanoclay loading.
v. Therefore, it can be suggested that the significant reinforcing effect of nanoclay and the improved HDT for PA 11 nanocomposites corresponds to the combination of high modulus and aspect ratio of nanoclay within the polymer matrix.

Acknowledgement

This work was funded by Universiti Malaysia Perlis, Athlone Institute of Technology and Ministry of Higher Education Malaysia.

REFERENCES

[1] L.S. Schadler, Polymer-based and Polymer-filled Nanocomposites, in Nanocomposite Science and Technology, P.M. Ajayan, L.S. Schadler, and P.V. Braun Eds. Weinhem: WILEY-VCH Verlag, 77-144 (2003).

[2] M. Okamoto, Polymer/Layered Silicate Nanocomposites (Rapra Review Reports, no. 14). Shrewsbury: Rapra Technology Limited, (2003).

[3] M. Alexandre, P. Dubois, Polymer-layered silicate nanocomposites: preparation, properties and uses of a new class of materials, Materials Science and Engineering: R: Reports **28**, 1-2, 1-63 (2000). DOI: https://doi.org/10.1016/s0927-796x(00)00012-7

[4] P.M. Ajayan, Nanocomposite Science and Technology, in Nanocomposite Science and Technology, P.M. Ajayan, L.S. Schadler, and P.V. Braun Eds. Weinheim: WILEY-VCH Verlag, 1-2, (2003).

[5] T.D. Fornes, D.R. Paul, Modeling properties of nylon 6/clay nanocomposites using composite theories, Polymer **44**, 17, 4993-5013 (2003). DOI: http://dx.doi.org/10.1016/S0032-3861(03)00471-3

[6] Y.-P. Wu, Q.-X. Jia, D.-S. Yu, L.-Q. Zhang, Modeling Young's modulus of rubber–clay nanocomposites using composite theories, Polymer Testing **23**, 8, 903-909 (2004).
DOI: http://dx.doi.org/10.1016/j.polymertesting.2004.05.004

[7] A. Zare-Shahabadi, A. Shokuhfar, S. Ebrahimi-Nejad, M. Arjmand, M. Termeh, Modeling the stiffness of polymer/layered silicate nanocomposites: More accurate predictions with consideration of exfoliation ratio as a function of filler content, Polymer Testing **30**, 4, 408-414 (2011).
DOI: https://doi.org/10.1016/j.polymertesting.2011.02.009

[8] S. Sinha Ray, M. Okamoto, Polymer/layered silicate nanocomposites: a review from preparation to processing, Progress in Polymer Science **28**, 11, 1539-1641 (2003).
DOI: 10.1016/j.progpolymsci.2003.08.002

[9] T. Kojima, Synthesis of Nylon-6-clay Hybrid by Montmorillonite Intercalated with epsilon-Caprolactam, ed. Japan, 983-986 (1993).

[10] A.A. Okada, J.P. Fukushima, Yoshiaki (Aichi, JP), Kawasumi, Masaya (Aichi, JP), Inagaki, Shinji (Aichi, JP), Usuki, Arimitsu (Aichi, JP), Sugiyama, Shigetoshi (Aichi, JP), Kurauchi, Toshio (Aichi, JP), Kamigaito, Osami (Aichi, JP), Composite material and process for manufacturing same, United States Patent 4739007, 1988. [Online].
Available: http://www.freepatentsonline.com/4739007.html

[11] J.I. Weon, H.J. Sue, Effects of clay orientation and aspect ratio on mechanical behavior of nylon-6 nanocomposite, Polymer **46**, 17, 6325-6334 (2005).
DOI: https://doi.org/10.1016/j.polymer.2005.05.094

[12] Y. Zare, K.Y. Rhee, S.-J. Park, A developed equation for electrical conductivity of polymer carbon nanotubes (CNT) nanocomposites based on Halpin-Tsai model, Results in Physics **14**, 102406 (2019).
DOI: https://doi.org/10.1016/j.rinp.2019.102406

[13] A. Navidfar, L. Trabzon, Graphene type dependence of carbon nanotubes/graphene nanoplatelets polyurethane hybrid nanocomposites: Micromechanical modeling and mechanical properties, Composites Part B: Engineering **176**, 107337 (2019).
DOI: https://doi.org/10.1016/j.compositesb.2019.107337

[14] E. Sadeghpour, Y. Guo, D. Chua, V.P.W. Shim, A modified Mori-Tanaka approach incorporating filler-matrix interface failure to model graphene/polymer nanocomposites, International Journal of Mechanical Sciences **180**, 105699 (2019). DOI: https://doi.org/10.1016/j.ijmecsci.2020.105699

[15] S. Korchagin, E. Romanova, D. Serdechnyy, P. Nikitin, V. Dolgov, V. Feklin, Modeling of Layered Nanocomposite of Fractal Structure, Mathematics **9**, 13, 1541 (2021).

[16] Y. Zhu et al., Investigation of the Constitutive Model of W/PMMA Composite Microcellular Foams, Polymers **11**, 7, 1136 (2019).

[17] S. Lhadi, M.-R. Chini, T. Richeton, N. Gey, L. Germain, S. Berbenni, "Micromechanical Modeling of the Elasto-Viscoplastic Behavior and Incompatibility Stresses of β-Ti Alloys, Materials **11**, 7, 1227 (2018).

[18] J. Scobbo, Thermomechanical Performance of Polymer Blends (Polymer Blends: Formulation and Performance). New York: John Wiley, 1987.

[19] C.L. Tucker Iii, E. Liang, Stiffness predictions for unidirectional short-fiber composites: Review and evaluation, Composites Science and Technology **59**, 5, 655-671 (1999). DOI: https://dx.doi.org/10.1016/S0266-3538(98)00120-1

[20] J.C.H. Affdl, J.L. Kardos, The Halpin-Tsai equations: A review, Polymer Engineering & Science **16**, 5, 344-352 (1976). DOI: https://doi.org/10.1002/pen.760160512

[21] K.C. Yung, J. Wang, T.M. Yue, Modeling young's modulus of polymer-layered silicate nanocomposites using a modified halpin - Tsai micromechanical model, Journal of Reinforced Plastics and Composites **25**, 8, 847-861 (2006).

[22] T. Mori, K. Tanaka, Average stress in matrix and average elastic energy of materials with misfitting inclusions, Acta Metallurgica **21**, 5, 571-574 (1973). DOI: http://dx.doi.org/10.1016/0001-6160(73)90064-3

[23] J. Wang, R. Pyrz, Prediction of the overall moduli of layered silicate-reinforced nanocomposites – part I: basic theory and formulas, Composites Science and Technology **64**, 7-8, 925-934 (2004). DOI: http://dx.doi.org/10.1016/S0266-3538(03)00024-1

[24] G.P. Tandon, G.J. Weng, The effect of aspect ratio of inclusions on the elastic properties of unidirectionally aligned composites, Polymer Composites **5**, 4, 327-333 (1984). DOI: https://doi.org/10.1002/pc.750050413

[25] http://prospector.ides.com/DataView.aspx, Rilsan BESVO A FDA

[26] http://www.scprod.com/product_bulletins/PB%20Cloisite%2030B.pdf, Cloisite 30B Typical physical properties bulletin